



PEARL

**Complete analysis of the B-cell response to a protein antigen, from *in vivo* germinal centre formation to 3-D modelling of affinity maturation**

Adams, CL; Macleod, MKL; James, Milner-White E; Aitken, R; Garside, P; Stott, DI

**Published in:**  
Immunology

**DOI:**  
[10.1046/j.1365-2567.2003.01583.x](https://doi.org/10.1046/j.1365-2567.2003.01583.x)

**Publication date:**  
2003

**Link:**  
[Link to publication in PEARL](#)

**Citation for published version (APA):**

Adams, CL., Macleod, MKL., James, MW. E., Aitken, R., Garside, P., & Stott, DI. (2003). Complete analysis of the B-cell response to a protein antigen, from *in vivo* germinal centre formation to 3-D modelling of affinity maturation. *Immunology*, *108*(3), 274-287. <https://doi.org/10.1046/j.1365-2567.2003.01583.x>

All content in PEARL is protected by copyright law. Author manuscripts are made available in accordance with publisher policies. Wherever possible please cite the published version using the details provided on the item record or document. In the absence of an open licence (e.g. Creative Commons), permissions for further reuse of content should be sought from the publisher or author.

## Complete analysis of the B-cell response to a protein antigen, from *in vivo* germinal centre formation to 3-D modelling of affinity maturation

CLAIRE L. ADAMS, MEGAN K. L. MACLEOD, E. JAMES MILNER-WHITE\*, ROBERT AITKEN†, PAUL GARSIDE & DAVID I. STOTT *Department of Immunology and Bacteriology, University of Glasgow, \*Division of Biochemistry and Molecular Biology, IBLS, University of Glasgow, Glasgow, and †Division of Infection and Immunity, IBLS, University of Glasgow, Glasgow, Scotland, UK*

### SUMMARY

Somatic hypermutation of immunoglobulin variable region genes occurs within germinal centres (GCs) and is the process responsible for affinity maturation of antibodies during an immune response. Previous studies have focused almost exclusively on the immune response to haptens, which may be unrepresentative of epitopes on protein antigens. In this study, we have exploited a model system that uses transgenic B and CD4<sup>+</sup> T cells specific for hen egg lysozyme (HEL) and a chicken ovalbumin peptide, respectively, to investigate a tightly synchronized immune response to protein antigens of widely differing affinities, thus allowing us to track many facets of the development of an antibody response at the antigen-specific B cell level in an integrated system *in vivo*. Somatic hypermutation of immunoglobulin variable genes was analysed in clones of transgenic B cells proliferating in individual GCs in response to HEL or the cross-reactive low-affinity antigen, duck egg lysozyme (DEL). Molecular modelling of the antibody–antigen interface demonstrates that recurring mutations in the antigen-binding site, selected in GCs, enhance interactions of the antibody with DEL. The effects of these mutations on affinity maturation are demonstrated by a shift of transgenic serum antibodies towards higher affinity for DEL in DEL-cOVA immunized mice. The results show that B cells with high affinity antigen receptors can revise their specificity by somatic hypermutation and antigen selection in response to a low-affinity, cross-reactive antigen. These observations shed further light on the nature of the immune response to pathogens and autoimmunity and demonstrate the utility of this novel model for studies of the mechanisms of somatic hypermutation.

### INTRODUCTION

Following antigen challenge, antigen-specific B cells enhance the 'quality', i.e. specificity and affinity, of the antibodies they produce over time. This process is important for protective immunity to pathogens and defects in this process lead to a profound susceptibility to bacterial infections.<sup>1,2</sup>

This improvement in antibody affinity and specificity takes place in the microenvironment of the germinal centre (GC) by the process of affinity maturation of B cell antigen receptors.<sup>3–5</sup> First, rearranged immunoglobulin (Ig) variable (V) region genes are mutated randomly in centroblasts within the dark zone of the

GC by a process known as somatic hypermutation.<sup>6–9</sup> Surface expression of these mutated Igs is up-regulated during differentiation of the centroblasts to centrocytes, which migrate to the light zone. Here they are preprogrammed to die by apoptosis unless they receive survival signals by ligation of the B cell receptor (BCR) with antigen which they encounter on the surface of follicular dendritic cells (FDCs). Competition for antigen results in selection of B cells with high affinity receptors. The surviving B cells receive further signals from CD4<sup>+</sup> helper T cells via their CD40 ligand and differentiate into either long-lived memory cells or antibody-producing plasma cells.<sup>3,10</sup>

Basic features of the hypermutation process have been deduced from the sequences of antibodies recovered from different stages of immune responses to a variety of antigens and haptens.<sup>11</sup> Single nucleotide substitutions are introduced in a stepwise manner into the Ig V region genes at an estimated rate of one mutation per 1000 base pairs (bp) per generation.<sup>6</sup> Mutations occur in both DNA strands<sup>12</sup> with a strong bias

Received 9 August 2002; revised 9 October 2002; accepted 12 November 2002.

Correspondence: Dr C. L. Adams, Department of Immunology and Bacteriology, University of Glasgow, Western Infirmary, Glasgow G11 6NT, Scotland, UK. E-mail: cla3r@clinmed.gla.ac.uk

for transitions over transversions<sup>8</sup> and the mutation machinery targets particular sequence motifs, or 'hot spots' of which the RGYW motif is best known.<sup>13–15</sup>

Somatic hypermutation in GCs has been studied primarily in mice responding to haptens, in which the response is dominated by single rearranged heavy and light chain V-genes.<sup>16–18</sup> It has been difficult to examine the germinal centre response to protein antigens directly *in vivo* due to the low precursor frequency and heterogeneity of B cells specific for a particular protein and the presence of multiple epitopes on the antigen, resulting in a response comprising a very heterogeneous population of rearranged V-genes.<sup>19</sup> In this study, we have exploited an adoptive transfer mouse model<sup>20</sup> which uses antigen receptor transgenic (Tg) B and CD4<sup>+</sup> T cells specific for hen egg lysozyme (HEL) and a chicken ovalbumin (cOVA) peptide, respectively, to investigate a tightly synchronized immune response to a protein antigen. Increasing the precursor frequency of T and B lymphocytes to defined epitopes in this model has greatly facilitated studies on B cell differentiation and migration into the lymphoid follicle,<sup>20,21</sup> receptor-editing of anergic B cells<sup>22</sup> and self/non-self B cell discrimination.<sup>23,24</sup>

The MD4 mouse strain<sup>23</sup> carries rearranged heavy and light chain transgenes which encode the HEL-specific monoclonal antibody, HyHEL-10, offering a unique opportunity to study B cell somatic hypermutation in germinal centres during the immune response to a protein antigen *in vivo*. We have exploited the fact that the HyHEL-10 antibody has approximately 3000 times lower affinity for duck egg lysozyme [ $K_a = 1.3 \times 10^7 \text{ M}^{-1}$  (25)] compared to HEL ( $K_a = 4.5 \times 10^{10} \text{ M}^{-1}$ ) but the MD4 Tg B cells are still able to expand in response to this lower-affinity antigen.<sup>26</sup>

The availability of the high resolution 3-D structures of HyHEL-10, its antigen and the antibody–antigen complex<sup>27–29</sup> has allowed us to use molecular modelling to study the effects of mutations in B cell clones proliferating within developing GCs. Molecular modelling of the HyHEL-10/DEL interface indicates that antigenic selection for mutations that enhance interactions with DEL specific residues is taking place within the GCs of DEL-cOVA immunized recipients. Selection of these mutations was accompanied by increased affinity of the transgenic antibodies for DEL.

To our knowledge, this is the first time that selection of replacement mutations in GC B cells responding to a protein antigen has been observed directly *in vivo* and their effects on the affinity of the antibody–antigen interaction followed through high resolution modelling of the receptor–antigen complex. This study expands our understanding of the individual and cumulative effects of somatic hypermutation on the binding of antibody to its epitope, leading to further insight into how the immune system combats infectious diseases by refinement of the antibody–antigen interaction during the evolution of the immune response.

## METHODS AND MATERIALS

### Preparation of DEL-cOVA and HEL-cOVA conjugates

Lysozyme was prepared from domestic duck eggs following the method described previously by Smith-Gill *et al.*<sup>30</sup> It was free of

contaminants, as determined by SDS-PAGE, and was shown to contain high specific activity by the *Micrococcus lysodeikticus* cell turbidimetric assay.<sup>31</sup>

Duck egg lysozyme or hen egg lysozyme (Biozyme Laboratories, Gwent, UK) was coupled to chicken ovalbumin (Sigma, Poole, UK) using glutaraldehyde (Sigma).<sup>20</sup>

### Mouse strains, adoptive transfer and immunization

D011.10 (BALB/c × C57BL/6) F<sub>1</sub> and MD4 (BALB/c × C57BL/6) F<sub>1</sub> transgenic (Tg) mice were used. All mice were bred and maintained in a specific pathogen-free facility at the University of Glasgow following home office regulations. D011.10 T cells express a Tg TCR specific for chicken ovalbumin peptide (323–329) in the context of I-A<sup>d</sup>.<sup>32</sup> Cell suspensions containing 1–2.5 × 10<sup>6</sup> D011.10 CD4<sup>+</sup> T cells and 2.5–5 × 10<sup>6</sup> MD4 B cells were transferred intravenously into (BALB/c-Igh<sup>b</sup> × C57BL/6)F<sub>1</sub> recipients.<sup>20</sup> After 1 day, HEL-cOVA or DEL-cOVA conjugate (130 µg) in complete Freund's adjuvant (CFA) was injected subcutaneously on the back. The Tg TCR was detected by the clonotypic monoclonal antibody KJ1-26.<sup>33</sup> MD4 B cells express the anti-HEL HyHEL-10 monoclonal antibody with both IgM and IgD isotypes<sup>23</sup> and can be identified using an antibody specific for the IgM<sup>a</sup> allotype. The percentage of CD4<sup>+</sup> KJ1-26<sup>+</sup> D011.10 T cells and B220<sup>+</sup> IgM<sup>a+</sup> MD4 B cells from the transgenic donors was determined by flow cytometry.

### Immunohistochemistry/FACS

The lymph nodes (brachial, axillary, cervical, inguinal and para-aortic) were harvested at specific time-points; half the lymph nodes from each recipient were used to prepare single cell suspensions and stained for flow cytometry as previously indicated.<sup>20</sup> FACS data were collected and analysed using FACS-calibur (Becton Dickinson, Oxford, UK) and the Cellquest software program, respectively.

The remaining lymph nodes were frozen in liquid nitrogen in OCT embedding medium (Miles, Elkurt, IN, USA) and stored at –80°. Tissue sections (6 µm) were mounted on precoated slides (Speci-Microsystems, Surrey, UK), fixed in acetone and stained with biotinylated anti-IgM<sup>a</sup>, HEL, DEL, peanut agglutinin (PNA) and anti-Thy1.2 as described previously.<sup>20</sup>

### Competitive ELISA

All reagents were diluted in ED buffer (0.2% fetal calf serum, 0.05% Tween 20 in PBS) unless stated otherwise. Sera from recipients were diluted and mixed with various quantities of hen egg lysozyme (1 µg/ml–5 pg/ml) or duck egg lysozyme (0.125 mg/ml–0.1 µg/ml) and incubated at 4° overnight. The titre of free anti-IgM<sup>a</sup> serum antibodies in solution was assayed by ELISA on plates (Immulon-4) coated with either 20 µg/ml DEL or HEL diluted in PBS. Detection was achieved using biotinylated anti-mouse IgM<sup>a</sup> (PharMingen, Oxford, UK) followed by extravidin peroxidase conjugate (Sigma).

### Microdissection, PCR amplification and cloning of the

#### HyHEL-10 light and heavy chain V transgenes

Germinal centres stained with the anti-allotype antibody IgM<sup>a</sup> and PNA (Vector, Burlingame, CA, USA) were excised by microdissection under Scott's tapwater substitute (0.35% NaHCO<sub>3</sub>,

**Table 1.** Oligonucleotide primers

Oligonucleotide name	Sequence (5'-3')
LL	TGGAYTYCAGCCTCCAGA
IL	TAACACCTGATCTGAGAATG
VL	GATATTGTGCTAACTCAGTCTCC
JL	TTATTCCAGCTTGGTCCC
LH	TGTTGACAGYCVTTCCCKGGT
IH	GTTGAATCTTGATTCCCGTT
VH	GTGCAGCTTCAGGAGTCAGGA
JH	TGCAGAGACAGTGACCAGAGT

0.2% MgSO<sub>4</sub>) using a Nikon Narishige micromanipulator. Photographs were taken with a Nikon Diaphot inverted microscope and a CCD camera. The tissue was digested in 30 µl of proteinase K (1.43 mg/ml; Boehringer Mannheim) for 1 hr at 50° followed by heat-inactivation at 95° for 10 min.

The HyHEL-10 heavy and light V(D)J transgenes were amplified by two rounds of polymerase chain reaction (PCR) using Expand<sup>TM</sup> DNA polymerase (Boehringer Mannheim, Indianapolis, IN, USA) and nested oligonucleotide primers (Table 1). To avoid contamination of reagents with amplified Ig V genes, all procedures before PCR took place in a separate laboratory from that where PCR amplification and all subsequent DNA manipulations were performed.

HyHEL-10 V $\kappa$  and VH genes contain 2 and 13 nucleotide differences from the closest germline genes, V $\kappa$ 23-43 and VH36-60, respectively.<sup>34</sup> The anti-lysozyme HyHEL-10 Ig heavy (H) chain gene construct consists of the LVDJ<sub>H</sub> gene segment,  $\mu$ -switch and constant regions,  $\mu$ -membrane exons, the  $\delta$ -constant, secretory and membrane gene segments. The anti-lysozyme HyHEL-10 Ig light (L) chain gene construct comprises the LVJ $\kappa$  gene segment and the  $\kappa$ -constant region. Both transgene constructs have been described in detail previously.<sup>23</sup> External 5' oligonucleotides (LL/LH) hybridized to relatively conserved motifs within the immunoglobulin signal sequences of the VH3 or V $\kappa$ 23 gene families.<sup>35</sup> The external 3' oligonucleotides (IH/IL) were specific for the intronic sequences immediately downstream from the JH3<sup>36</sup> or J $\kappa$ 2<sup>37</sup> gene segments. Internal oligonucleotides (VL/JL, VH/JH) were complementary to the 5' or 3' ends of the rearranged HyHEL10 light and heavy chain V regions, respectively.<sup>34,38</sup>

The HyHEL-10 light chain V-gene was amplified using the external oligonucleotides LL and IL followed by internal primers VL and JL. The HyHEL-10 heavy chain V-gene segment was amplified with external oligonucleotides LH and IH followed by internal primers VH and JH.

The cycling parameters for the PCRs were: 95°, 2 min; (94°, 1 min, 55°, 1 min, 72°, 2 min)  $\times$  40; 72°, 15 min except that the annealing temperature was 52° for the primary amplification of the HyHEL-10 light chain V-gene. A wax-gem (Perkin-Elmer, Norwalk, CT, USA) facilitated hot start was used in all PCRs.

Ten microlitres of the digested tissue was used in all primary amplification PCRs and 2 µl of the primary PCR product was used in the second amplification step. Negative control samples containing water instead of DNA were always amplified in

parallel with the DNA from the digested tissue. PCR products were purified using either a Qiaquick gel extraction kit or a PCR purification kit (Qiagen, Sussex, UK), ligated into plasmid vector pCR2 and cloned using the TA cloning system (Invitrogen, Paisley, UK).

#### *Sequencing and analysis of the HyHEL-10 light and heavy chain V region transgenes*

Plasmid DNA was isolated from single clones and positive transformants were chosen at random for automated DNA sequencing (DNASHEF, Edinburgh, UK). Sequence chromatographs were analysed with Editview and alignments were carried out by DNAPlot. The MD4 B cells contain four copies of the transgene; one copy contains a silent mutation at amino acid position 45 of the V $\kappa$  region<sup>39</sup> and was eliminated from any mutational analysis. Dendrograms were produced using sequences with shared subsets of somatic mutations cloned from individual germinal centres; each unique sequence represents the B cell expressing that mutated V-gene.

## RESULTS

### **Kinetics of the DEL-cOVA response**

To ensure that DEL coupled to cOVA can elicit B cell help from TCR Tg T cells, as reported previously for HEL, we examined the clonal expansion of Tg T and B cells. HEL-specific Tg B cells and OVA-specific TCR T cells were transferred into naive congenic (BALB/c-Igh<sup>b</sup>  $\times$  C57BL/6) F<sub>1</sub> mice, which were then immunized with either HEL-cOVA or DEL-cOVA in CFA. The lymph nodes were removed from the recipients at days 3, 5, 7, 9 and 14 after immunization, and cells from half the lymph nodes were analysed by flow cytometry. The remaining lymph nodes were used for immunohistochemical analysis. Clonal expansion of both the Tg D011.10 T and MD4 B cells in response to the lower-affinity conjugate, DEL-cOVA, was detected *in vivo*. As shown in our previous studies<sup>20,21</sup> the peaks of clonal expansion in response to the high-affinity HEL-cOVA conjugate were observed on days 3 and 5 for the Tg T and B cells, respectively (Fig. 1). In contrast, following immunization with DEL-cOVA, the expansion of Tg OVA-specific T cells was slower than observed in response to the higher affinity, HEL-cOVA. This suggests that B cells present DEL-acquired cOVA less efficiently to T cells at the earlier stages of GC formation due to their lower affinity for DEL-cOVA<sup>40</sup> or, alternatively, that the two antigens are presented by phenotypically distinct antigen-presenting cells. There was no significant delay in the B cell response to DEL-cOVA compared to HEL-cOVA. This observation is in agreement with a recent finding that high- and low-affinity B cells have the same intrinsic capacity to respond to antigen.<sup>41</sup> These results demonstrate that the MD4 B cells respond to DEL while receiving help from the D011.10 T cells.

### **Localization of Tg MD4 B cells and D011.10 T cells during the DEL-cOVA response**

Following immunization, antigen-specific T cells undergo clonal expansion and migrate into B cell follicles, where they

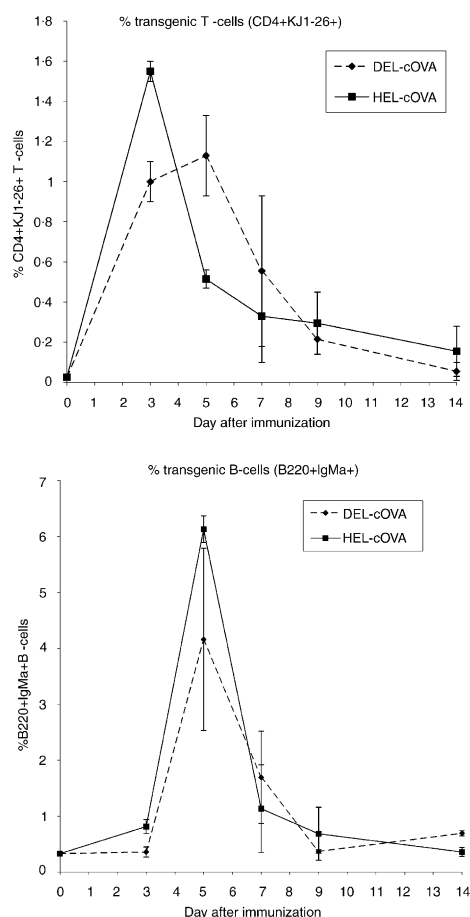


**Figure 1.** Kinetics of D011-10 T and MD4 B cell clonal expansion after immunization. Cell suspensions containing  $1-5 \times 10^6$  CD4<sup>+</sup>KJ1-26<sup>+</sup> T cells and B220<sup>+</sup> HEL<sup>+</sup> B cells were transferred into BALB/c-Igh<sup>b</sup> × C57BL/6 F<sub>1</sub> mice. On day 0, transferred recipients were injected s.c. with either 130 µg of HEL-cOVA or DEL-cOVA in CFA. The percentage of (a) D011-10 (CD4<sup>+</sup>KJ1-26<sup>+</sup>) T cells and (b) MD4 (B220<sup>+</sup>IgMa<sup>+</sup>) B cells in the lymph nodes of adoptively transferred recipients were determined by flow cytometry at days 3, 5, 7, 9 and 14 after immunization. Each time-point represents the mean ± range for at least two mice per group. Unimmunized controls from each time-point were averaged and represented as day 0.

provide help to B cells.<sup>20,21</sup> Similar follicular migration for both the Tg B and T cells was displayed in both the DEL-cOVA and HEL-cOVA immunized recipients. PNA-positive GCs containing transgenic IgM<sup>+</sup> B cells were observed at days 5–14 with both the high (HEL)- and low (DEL)-affinity antigens by immunohistochemistry (Fig. 2) and three-colour flow cytometry (unpublished data). Although numerous anti-HEL-specific Tg B cells were detected (Fig. 2a,b) within the GCs of both HEL-cOVA and DEL-cOVA immunized mice, no DEL-binding B cells were detected in the GCs of the DEL-immunized mice (Fig. 2c). The inability to detect DEL-binding B cells may be due to the sensitivity of the immunochemical system employed. We have established a system in which affinity maturation of a trackable population of antigen-specific B cells can be analysed during the germinal centre reaction *in vivo*.

### Somatic hypermutation in germinal centres responding to DEL and HEL

The V<sub>K</sub> and V<sub>H</sub> region transgenes were amplified by nested PCR from 12 IgM<sup>+</sup>, PNA<sup>+</sup> GCs at various stages of the primary response to both HEL-cOVA and DEL-cOVA. The GCs were identified by PNA staining and consisted of approximately 400–600 cells. Care was taken to avoid the inclusion of PNA negative/non-transgenic B cells in the surrounding area.

The average mutation rate in the germinal centres for both the HEL-cOVA and DEL-cOVA immunized mice was fairly similar, ranging from 0.3 to 0.5% (Table 2).

There was extensive variability in the mutation rate between germinal centres with the occasional GC displaying no mutations within the sample of transgenes analysed. This supports previous findings that substantial clonal expansion within germinal centres can occur without activation of the hypermutation mechanism,<sup>42,43</sup> although other reports have suggested that ongoing mutation may occur in all GCs.<sup>44,45</sup> Inactivation of the hypermutation machinery may be advantageous at the early stages of germinal centre formation since the accumulation of deleterious mutations within the GC founder cells would be detrimental.

Intrinsic mutational hotspots encoded by an RGYW motif (R = A or G, Y = C or T, W = A or T)<sup>8,14</sup> were observed within the V<sub>H</sub> and V<sub>K</sub> region transgenes of GCs from HEL-cOVA and DEL-cOVA immunized recipients (Fig. 3). Mutations at these hotspots tend to produce conservative coding changes such as serine to asparagine/threonine, hence preserving antibody structure. Additionally, the somatic hypermutation machinery displays a strong bias of transitions over transversions (59% compared with the 33% anticipated on a random bias);<sup>8</sup> 60% of the mutations were transitions in this experimental system. These results indicate that somatic hypermutation of the antigen-specific B cells was occurring in a primary immune response to a protein antigen *in vivo*.

### Clonal proliferation within GCs

Reconstruction of the hypermutation and clonal expansion events that took place in each GC was undertaken using a previously established procedure for building genealogical dendrograms (Fig. 4).<sup>42,44</sup>

Potentially affinity-enhancing mutations were retained through a number of cell divisions in some B cell clones (Fig. 4a,b). This may reflect a situation where B cells with antigen-enhancing mutations are being selected and recirculating for additional rounds of somatic mutation (branching dendrograms). Many GCs at days 9 and 14 from the HEL-cOVA and DEL-cOVA immunized recipients displayed mutationally distinct B cells emanating from the unmutated transgenes. These dendrograms are described as simple (Fig. 4c) where a number of B cells containing one or two mutations but no shared mutations were observed. These simple dendrograms suggest that there is an ongoing emigration of B cells leaving the GC without further rounds of division and mutation. The fact that the transgenic B cells already have moderate affinity for DEL and high affinity for HEL may explain this observation.

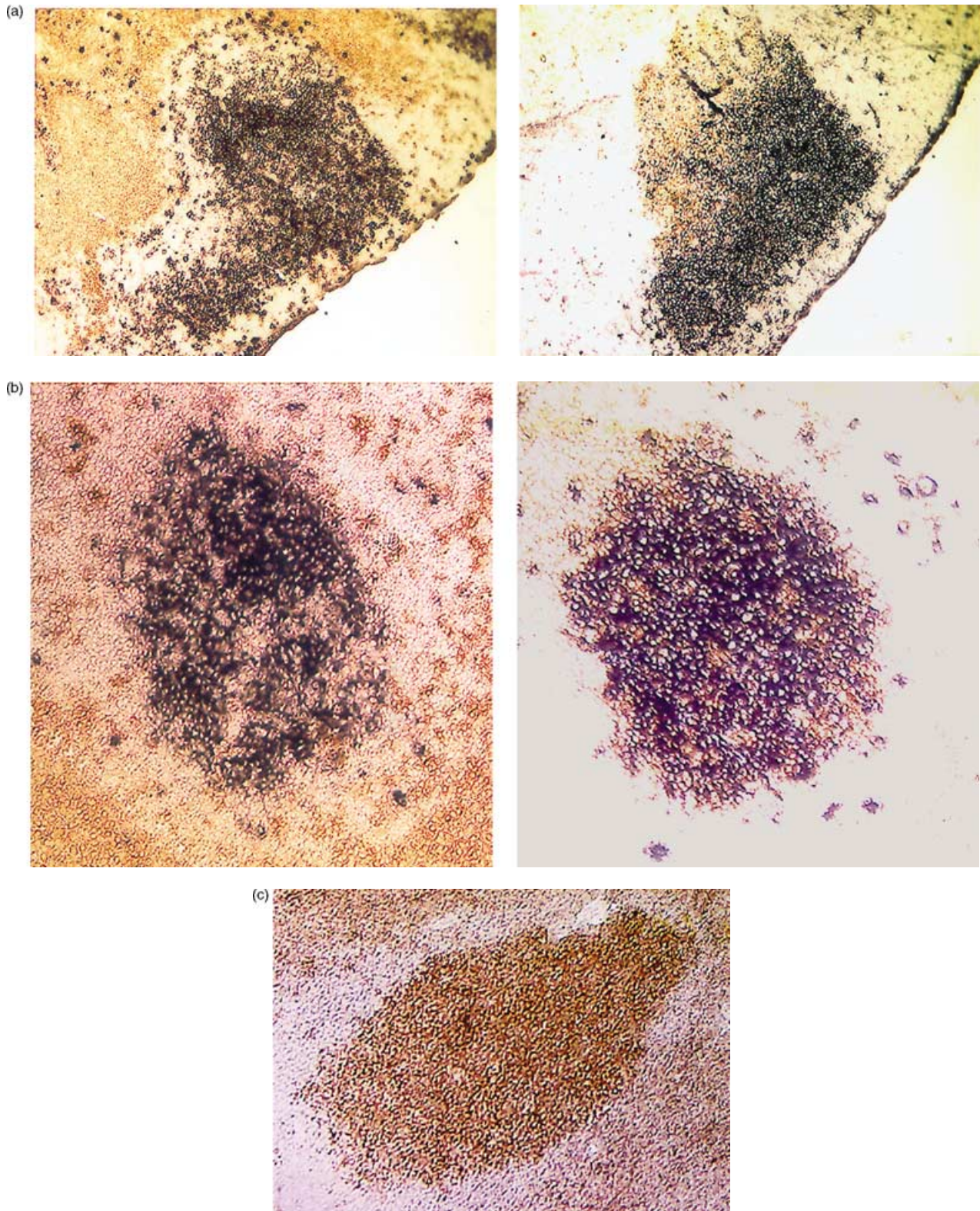


**Figure 2.** Immunohistochemical analysis of GCs in lymph nodes of HEL-cOVA and DEL-cOVA immunized mice. The consecutive sections were stained with either anti-Thy1.2 (brown) or peanut agglutinin (PNA) and either anti-IgM<sup>a</sup>, HEL or DEL (blue). Magnification was at  $\times 100$ . (a) Germinal centre from a HEL-cOVA immunized mouse, d9, IgM<sup>a+</sup> Thy1.2<sup>+</sup> (left) and HEL<sup>+</sup>PNA<sup>+</sup> (right). (b) Germinal centre from a DEL-cOVA immunized mouse, d9, IgM<sup>a+</sup>Thy1.2<sup>+</sup> (left) and HEL<sup>+</sup>PNA<sup>+</sup> (right). (c) Germinal centre from a DEL-cOVA immunized mouse, d9, DEL<sup>-</sup> PNA<sup>+</sup>.

**Table 2.** Summary of sequencing results obtained from individual GCs at different days after immunization with DEL-cOVA or HEL-cOVA

GC	Day	V gene	Description of B-cell clones	No. of unique sequences	No. of mutations	% unmutated transgenes
A. DEL-cOVA immunized mice						
B	5	H	Simple	5	6	63.6 (7/11)*
		L	Branching	5	7	55.5 (5/9)
D	5	H	Simple	3	2	81.8 (9/11)
		L	Simple	4	5	42.9 (3/7)
A	9	L	Branching	4	7	20 (1/5)
		H	Extensive branching	9	13	33.3 (3/9)
J	9	H	Simple	4	5	0 (0/7)
L	9	H	No SM†	1	0	100 (6/6)
		L	Extensive	7	14	38.5 (5/13)
A	14	H	Branching	1	0	100 (11/11)
		L	No SM	1	0	100 (11/11)
B. HEL-cOVA immunized mice						
C	9	L	Branching	11	15	41.2 (7/17)*
		H	Branching	9	18	43.8 (7/16)
F	9	L	Simple	4	6	30 (3/10)
G	9	L	Simple	7	6	40 (4/10)
D	14	H	Simple	4	4	70 (7/10)
K	14	L	Simple	4	3	40 (4/10)

(A) Average VL mutation rate = 0.49%; average VH mutation rate = 0.32%. (B) Average VL rate = 0.36%; average VH rate = 0.5%.

Results obtained from the analysis of primary GCs over days 5, 9, and 14. Data from individual GCs are shown on separate lines. The number of unique somatic mutations per GC was evaluated by counting mutations shared by two or more VH/VL clones only once. Average mutation frequency per V-gene base pair was calculated by dividing total number of somatic mutations observed by the total number of base pairs sequenced. Dendrograms containing a number of mutationally distinct B cells emanating from the unmutated transgene were described as simple. A branching dendrogram represents a number of B cells with shared and unique mutations, which can be followed along one arm of the dendrogram.

\*The number of unmutated transgenes in the total number of sequences analysed is shown in parentheses.

†No SM = no mutations were observed.

Neighbouring GCs from the same section of lymph node were also examined in two cases and no sequences with shared mutations were observed (unpublished data). This is in agreement with previous work suggesting that little or no inter-GC B cell migration takes place and that somatic hypermutation occurs completely independently in individual GCs.<sup>45,46</sup>

### Affinity maturation towards DEL

Changes in the relative affinity of the HyHEL-10 antibody for DEL and HEL were measured by competitive inhibition. Sera from adoptively transferred recipients immunized with either HEL-cOVA or DEL-cOVA were analysed at days 9 and 14. HyHEL-10 antibodies in the sera of DEL-immunized mice consistently showed increased affinity for DEL, both in solution (Fig. 5a) and in solid phase (Fig. 5b), compared with sera from HEL-immunized mice. A unique population of DEL-specific Tg antibodies, which could not be inhibited at high concentrations of HEL, was detected in the sera of DEL-cOVA immunized mice (Fig. 5b). These results provide evidence that somatic hypermutation within the V $\kappa$  and VH region transgenes resulted in increasing affinity for DEL in response to immunization with DEL-cOVA.

### Protein modelling of the affinity maturation process

High-resolution structural characterization of the HyHEL-10/HEL interaction<sup>27–29</sup> has allowed the examination of individual

replacement mutations that have occurred within this experimental system. Crystallography studies have identified 14 hydrogen bonds, 111 Van der Waals contacts and one salt bridge within the interface of the HyHEL-10/HEL complex.<sup>28</sup> The shape of the antigen-binding site is a very shallow concavity consisting of acidic and non-hydrophobic residues, bordered by hydrophobic segments.<sup>27</sup> There are 21 differences between the amino acid sequence of HEL and DEL (at positions 3, 4, **15**, 33, 34, 37, 57, 68, **73**, **75**, **77**, 82, 85, 90, 91, 92, **93**, **97**, 116, 121, 122; 22 in *Duck form III*),<sup>25</sup> and these amino acids changes were modelled using the SwissPdb viewer version 3-3b3.

Of the 21 differences between HEL and DEL, six (in bold type, above) lie at the antigen-antibody interface, by inference from the HyHEL-10/HEL structure. All six occur in one half of the antibody interface: CDR2(L), CDR1(H) plus CDR3(H) and not CDR2(H), CDR1(L) or CDR3(L). This is illustrated in Fig. 6g.

This leads to an enquiry as to whether any of these six residues are near to any of the antibody residues that mutate during the affinity maturation process *in vivo*. The answer is one of them, namely residue 93. In HEL, residue 93 is an asparagine whose side chain is specifically hydrogen-bonded to the side chain of the 53V $\kappa$  glutamine, as seen in Fig. 6a. In DEL, residue 93 is an arginine, with a side chain of different hydrogen bond specificity.

Nearby, a striking feature of the antigen-binding site in the HyHEL-10/HEL complex is the 49V $\kappa$  lysine, which is prominently exposed and accessible at the centre.<sup>27</sup> This residue was

		CDR1											CDR2											CDR3												
		24	25	26	27	28	29	30	31	32	33	44	45	46	47	48	49	50	51	52	53	54	55	56	74	75	76	77	89	90	91	92	93	94	95	96
Light	HyHEL10	R	A	S	Q	S	I	<b>G</b>	<b>N</b>	<b>N</b>	L	P	R	L	L	I	K	<b>Y</b>	A	S	<b>Q</b>	S	I	S	S	I	N	S	<b>Q</b>	<b>Q</b>	<b>S</b>	<b>N</b>	S	W	P	<b>Y</b>
		AGG	GCC	AGC	CAA	AGT	ATT	GGC	AAC	AAC	CTA	CCA	AGG	CTT	CTC	ATC	AAG	TAT	GCT	TCC	CAG	TCC	ATC	TCT	AGT	ATC	AAC	AGT	CAA	CAG	AGT	AAC	AGC	TGG	CCG	TAC
DAY 5	15D	---	---	---	---	---	---	---	---	---	---	---	---	---	---	---	---	---	---	---	---	---	---	---	---	---	---	---	---	---	---	---	---	---	---	
DEL-cOVA	16D	---	---	---	---	---	---	---	---	---	---	---	---	---	---	---	---	---	---	---	---	---	---	---	---	---	---	---	---	T	D	---	---	---	---	
DAY 9	1A	---	---	---	---	---	---	---	---	---	---	---	---	---	---	---	N	---	---	---	---	---	---	---	---	---	---	---	---	---	---	---	---	---	---	
DEL-cOVA	3A	---	---	---	---	F	---	---	---	---	---	S	---	---	---	---	---	---	---	---	---	---	---	---	---	---	---	---	---	---	---	---	---	---	---	
	1H	---	---	---	---	T	---	---	---	---	---	T	---	---	---	---	---	---	---	---	---	---	---	---	---	---	---	---	---	T	---	---	---	---	---	
	1A	---	---	---	---	---	---	---	---	---	---	---	---	---	---	---	---	---	---	---	---	---	---	---	---	N	---	---	---	---	---	---	---	---	---	
DAY 14	13A	---	---	---	---	---	---	---	---	---	---	---	---	---	---	---	---	---	---	---	---	---	---	---	---	---	---	---	R	---	---	---	---	I	---	
DEL-cOVA	14A	---	---	---	---	---	---	---	---	---	---	---	---	---	---	---	M	---	---	---	---	---	---	---	---	---	---	---	-G	---	---	---	---	-T	---	
	20A	---	---	---	---	---	---	---	---	---	---	---	---	---	---	---	-T	---	---	---	---	---	---	---	---	---	---	---	---	---	---	---	---	N	---	
DAY 9	9C	---	---	---	---	---	---	---	---	---	---	S	---	---	---	---	---	---	---	---	---	---	---	---	---	---	---	---	---	---	---	---	---	---	---	
HEL-cOVA	19C	---	---	---	---	F	---	---	S	---	---	T	---	---	---	---	---	---	---	---	---	---	---	---	---	---	---	---	---	---	---	---	---	R	---	
	11G	---	---	---	---	---	---	---	---	---	---	---	---	---	---	---	---	---	---	---	---	---	---	---	---	---	---	---	---	-G	---	---	---	---	---	
(b)		CDR1					CDR2											CDR3																		
		30	31	32	33	34	35	50	51	52	53	54	55	56	57	58	59	60	61	62	63	64	98	99	100	101	102									
Heavy	HyHEL-10	T	S	D	Y	W	S	<b>Y</b>	V	<b>S</b>	<b>Y</b>	<b>S</b>	G	<b>S</b>	T	<b>Y</b>	Y	N	P	S	L	K	<b>W</b>	D	G	D	Y									
		ACC	AGT	GAT	TAT	TGG	AGC	TAC	GTA	AGC	TAC	AGT	GGT	AGC	ACG	TAC	TAC	AAT	CCA	TCT	CTC	AAA	TGG	GAC	GGT	GAT	TAC									
DAY 5	7B	---	---	---	---	---	---	---	---	---	---	---	---	---	---	---	---	---	---	---	---	---	---	---	---	---	---									
DEL-cOVA		---	---	---	---	---	---	---	---	---	---	---	---	---	---	---	---	---	---	---	---	---	---	---	---	---	---									
DAY 9	2H	---	---	---	---	---	---	---	---	---	---	S	N	---	---	---	---	---	---	---	---	---	---	---	---	---	---									
	7H	---	---	---	---	---	---	---	---	---	---	A	-A	---	---	---	---	---	---	---	---	---	---	---	---	---	---									
DEL-cOVA		---	---	---	---	---	---	---	---	---	---	---	N	---	---	---	---	---	---	---	---	---	---	---	---	---	---									
	11H	---	---	---	---	G	---	---	---	---	---	---	---	---	---	---	---	---	---	---	---	---	---	---	---	---	---									
	15H	---	---	---	---	G	---	---	---	---	---	---	---	---	---	---	---	---	---	---	---	---	---	---	---	---	---									
	6D	---	---	---	---	C	---	---	---	---	---	---	---	---	---	---	---	---	---	---	---	---	---	---	---	---	---									
DAY 9	13C	---	---	---	---	---	---	---	---	---	---	---	---	---	S	---	---	---	---	---	---	---	---	---	---	---	---									
	15C	---	---	---	---	---	---	---	---	---	---	---	---	---	T	---	---	---	---	---	---	---	---	---	---	---	---									
HEL-cOVA		---	---	---	---	---	---	---	---	---	---	---	---	---	S	---	---	---	---	---	---	---	---	---	---	---	---									
	20c	---	---	---	---	---	---	---	---	---	---	---	---	---	T	---	---	---	---	---	---	---	---	---	---	---	---									
		---	---	---	---	---	---	---	---	---	---	---	---	---	H	---	---	---	---	---	---	---	---	---	---	---	---									
		---	---	---	---	---	---	---	---	---	---	---	---	---	C	---	---	---	---	---	---	---	---	---	---	---	---									

**Figure 3.** Representative examples of the V $\kappa$  and V $\text{H}$  sequence data obtained from GCs at various stages of the HEL-cOVA/DEL-cOVA response. Each sequence is compared to the relevant HyHEL-10 transgene: (a) V $\kappa$ ; (b) V $\text{H}$ . Sequences of CDR1/CDR2 and CDR3 are completely shown as well as the flanking sections where somatic mutation was observed. Identity with the transgene is indicated by a dash and nucleotide differences are shown. The number of days after immunization and the antigen used are indicated in the left hand column. Numbers in front of the sequence alignment are arbitrary sequence names and the letter depicts the different isolated germinal centres. The CDRs in this figure are labelled according to Lavoie *et al.* 1999<sup>34</sup> and the amino acids in bold represent contact residues.



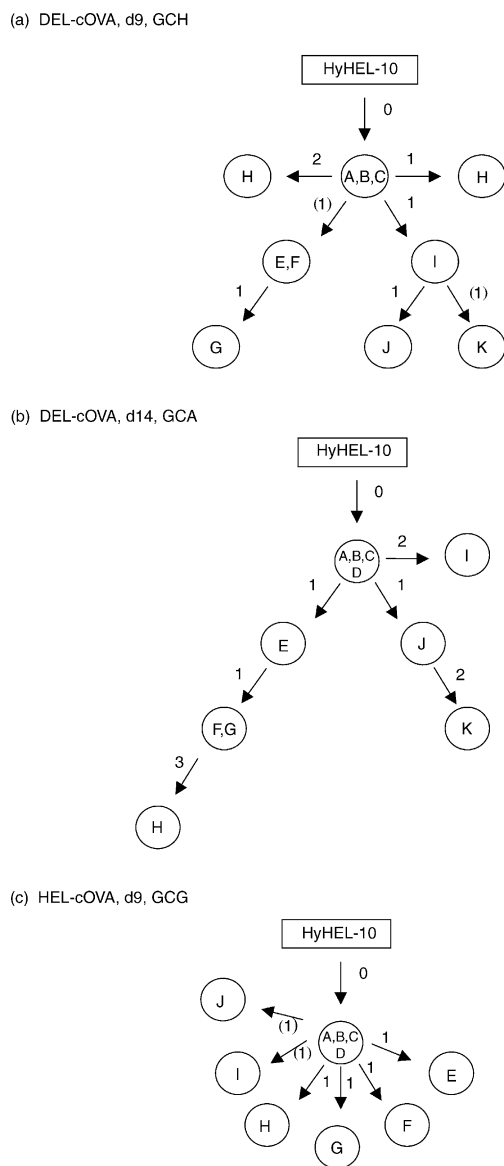


**Figure 4.** Clonal proliferation of B cells within individual GCs. A simplified hypothesis that each V-gene containing a unique set of mutations represents a distinct GC B cell was made. Each branch of the dendrogram represents mutations that were shared by several V-genes, using the assumption that the mutation event occurred only once in a precursor cell and was inherited by daughter cells. Numbers on branches represent the number of mutations (silent mutations are enclosed in brackets) between the different sequences. Each circle symbolizes a B cell and letters within the circles depict individual sequences. Branching dendrograms represent VH (a) and V $\kappa$  (b) sequences derived from independent GCs from days 9 and 14, respectively, in the DEL-cOVA response. The VH antigen-selected hotspot Ser56 $\rightarrow$ Asn is symbolized by B cells, I, J and K on the right-hand side of the dendrogram (a). The 'affinity-enhancing' mutation Lys49 $\rightarrow$ Met of VL is depicted by letters E, F, G and H on the left-hand side of the dendrogram (b), and B cell, H, also contains the intrinsic hotspots, Ser77 $\rightarrow$ Ile and Ser91 $\rightarrow$ Asn. (c) depicts a simple dendrogram produced from the V $\kappa$  sequence data from a HEL-cOVA GC.

seen to mutate independently in GC B cells to an asparagine or a methionine at days 9 and 14, respectively (Fig. 3a). The functional importance of these somatic mutations at residue 49V $\kappa$  was indicated by modelling of the HyHEL-10/DEL interface (Fig. 6b,c). The asparagine produced by point mutation at residue 49V $\kappa$  interacts directly, via hydrogen-bonding, with the DEL-specific amino acid, arginine 93 mentioned above. The methionine at 49V $\kappa$  may also result in enhanced binding to DEL through donation of electrons by the sulphur of the methionine to the guanidino group of arginine 93 (Fig. 6c). The importance of this position for antigen binding has been demonstrated by site-directed mutagenesis studies in which conversion of the lysine at residue 49V $\kappa$  to a threonine increased the affinity of the HyHEL-10 antibody for duck egg lysozyme approximately fivefold.<sup>25</sup> It is remarkable that the predicted importance of mutations at this position has been confirmed in an antigen-specific B cell response *in vivo*.

At the rest of the antibody-antigen interface where residue changes between HEL and DEL are not seen, some  $\kappa$  chain mutations were found in GC B cells. The serine to asparagine replacement mutation at position 93V $\kappa$  in CDR3 (Fig. 3a), also previously examined by site-directed mutagenesis, does not significantly alter affinity for DEL, at least in the presence of threonine at residue 49V $\kappa$ .<sup>25</sup> Protein modelling of this mutation, which is next to a contact residue, displays no alteration in hydrogen bonding within the Ag-Ab interface. Thr/Asn/Asp/Ser amino acids often occur in similar hydrogen bonding arrangements and, in such situations, can be considered interconvertible.<sup>47,48</sup>

Serine 91V $\kappa$  of the light chain, which is a contact residue in CDR3 with the HEL and DEL amino acid tyrosine 20, is believed to be a mutational hotspot. Conserved coding changes from serine 91V $\kappa$  to asparagine or threonine were observed at days 5, 9 and 14 in DEL-cOVA responding GCs only (Fig. 3a) and modelling suggests the possibility of maintenance of interactions with Tyr20. The V $\kappa$  transgenes from DEL-cOVA immunized mice showed a very high preference for transition replacements, particularly in CDR3, which may reflect the requirement for modification to increase interactions with the lower affinity antigen, DEL. This is surprising, because most of the non-identical DEL residues at the Ag-Ab interface are interacting with CDR2(L) and HEL/DEL residues close to CDR3(L) are identical.

Mutations in the framework regions, notably at serine residues 74V $\kappa$  and 77V $\kappa$  in the light chain of monoclonal antibody, HyHEL-8, were also observed in this experimental system. These are considered to be intrinsic hotspots within the light chain nucleotide sequence with conservative coding changes that preserve the antibody structure and are unlikely to affect antigen/antibody interactions.

Overall, the variable heavy chain transgene displayed a lower level of mutation compared with the light chain, with no mutations shared between independent GCs from the HEL-cOVA and DEL-cOVA GCs (Fig. 3b). Protein modelling of the mutation of the CDR2 contact residue serine 56VH to asparagine, which was observed at day 9 in a DEL-cOVA GC, showed an enhanced hydrogen-bond interaction with the lysozyme amino acid, aspartic acid 101, which is present in both the HEL and DEL. This mutation also occurs within the HyHEL-8 antibody, which displays higher affinity for DEL.<sup>25</sup>

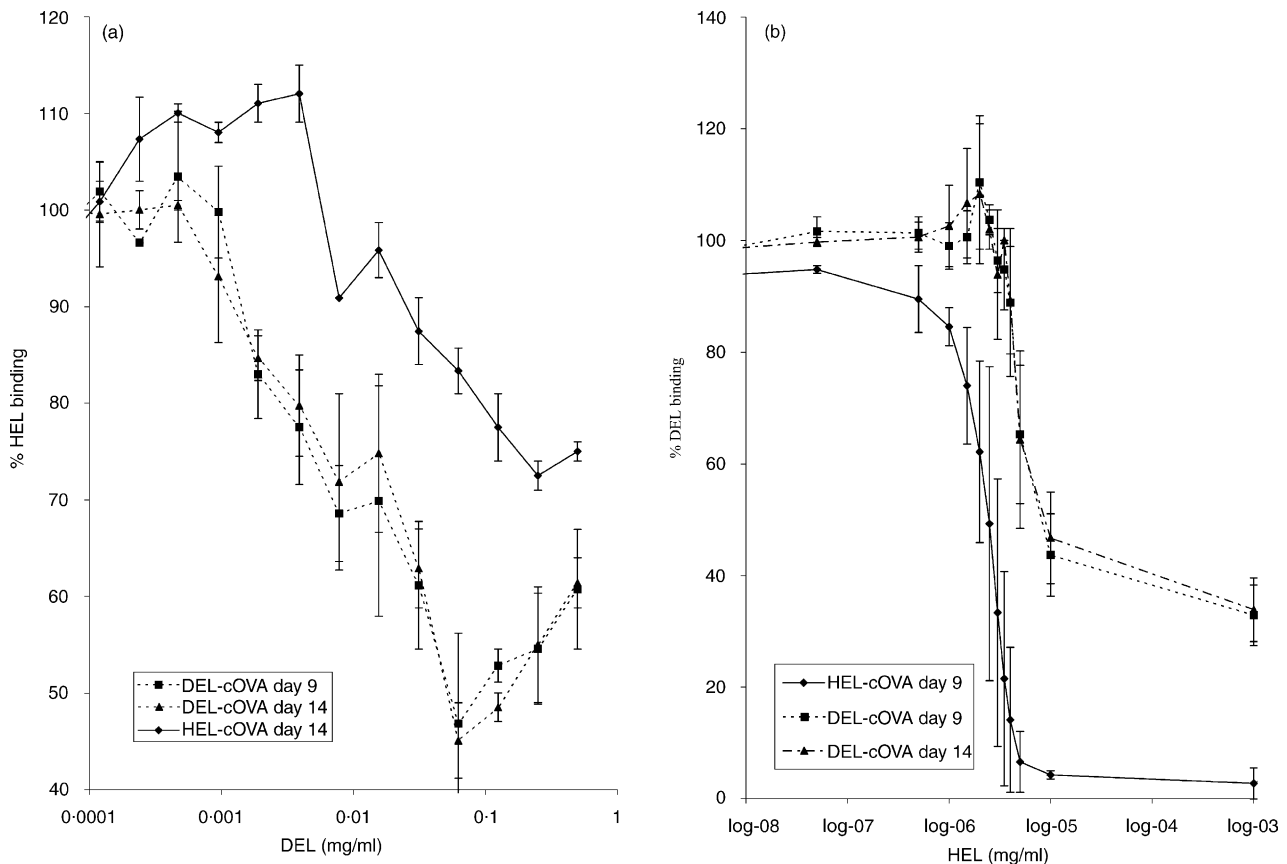


**Figure 5.** Relative affinity of IgM<sup>d</sup> transgenic antibodies in sera from HEL-cOVA and DEL-cOVA immunised recipients at days 9 and 14, by competitive ELISA. (a) Competitive binding of IgM<sup>d</sup> antibodies to HEL (solid phase) by DEL (soluble phase); (b) competitive inhibition of IgM<sup>d</sup> antibodies to DEL (solid phase) by HEL (soluble phase); average of two identical experiments.

Protein modelling of the other coding changes within and around the CDRs typically displayed conserved mutations, which are unlikely to have a major impact on antigen/antibody interaction. As no recurring mutations were observed we cannot rule out the possibility that some of these individual mutations may have resulted from PCR error.

Significantly, no coding changes were detected at the heavy chain residue, aspartic acid 32VH that is essential for maintaining the salt bridge to lysine/arginine 97 at the HEL and DEL interface, respectively. Additionally, little mutation was observed in the lower portion of the antigen binding site that is dominated by a cluster of tyrosine residues over the L3 and H2 areas. These Tyr amino acids are believed to create more favourable Ag–Ab interactions through their clustering effectively preventing contact of any other surrounding residues from direct interaction with HEL.<sup>27,49</sup>

#### Comparison of patterns of somatic mutation between HEL and DEL-cOVA immunized mice

Comparison of the total sequence data from GCs of mice immunized with DEL-cOVA and HEL-cOVA revealed different patterns of replacement mutations. Coding changes such as the mutations at 49V $\kappa$ , which increase binding to DEL, were not

detected in GCs responding to HEL. Since most of the unshared DEL residues were in the vicinity of CDR2(L), CDR3(H) and CDR1(H), one might predict a larger number of affinity-enhancing mutations in that half of the antibody interface. This was not observed, possibly because any bias would be small due to sample size.

Three light chain mutations were repeated in distinct GCs responding to HEL and DEL. It is unlikely that these mutations could have occurred at random and therefore are likely to have been selected during the GC response. Protein modelling indicated that two of the residues at these sites, Ile29 and Gln90, are essential for the conservation of the structure of the canonical loops.<sup>50,51</sup> According to the canonical class alignment definitions, residue 29 is allowed to be a Val or a Ile, to maintain the class 2 L1 loop and the amino acid at position 90 must be either a Gln, Asn or a His amino acid to preserve the class 1 L3 loop structure.<sup>52</sup> Modelling of the mutations (IleV $\kappa$ 29→Phe and GlnV $\kappa$ 90→Arg) indicated that they were energetically unfavourable, and were likely to make a structural change in the loop. These canonically important residues were observed to mutate simultaneously with other local amino acids in the same CDR (IleV $\kappa$ 29→Phe with AsnV $\kappa$ 32→Ser, GlnV $\kappa$ 90→Arg with SerV $\kappa$ 93→Ile), suggesting that, the local mutations observed in CDRL1 and CDRL3 could be compensating for

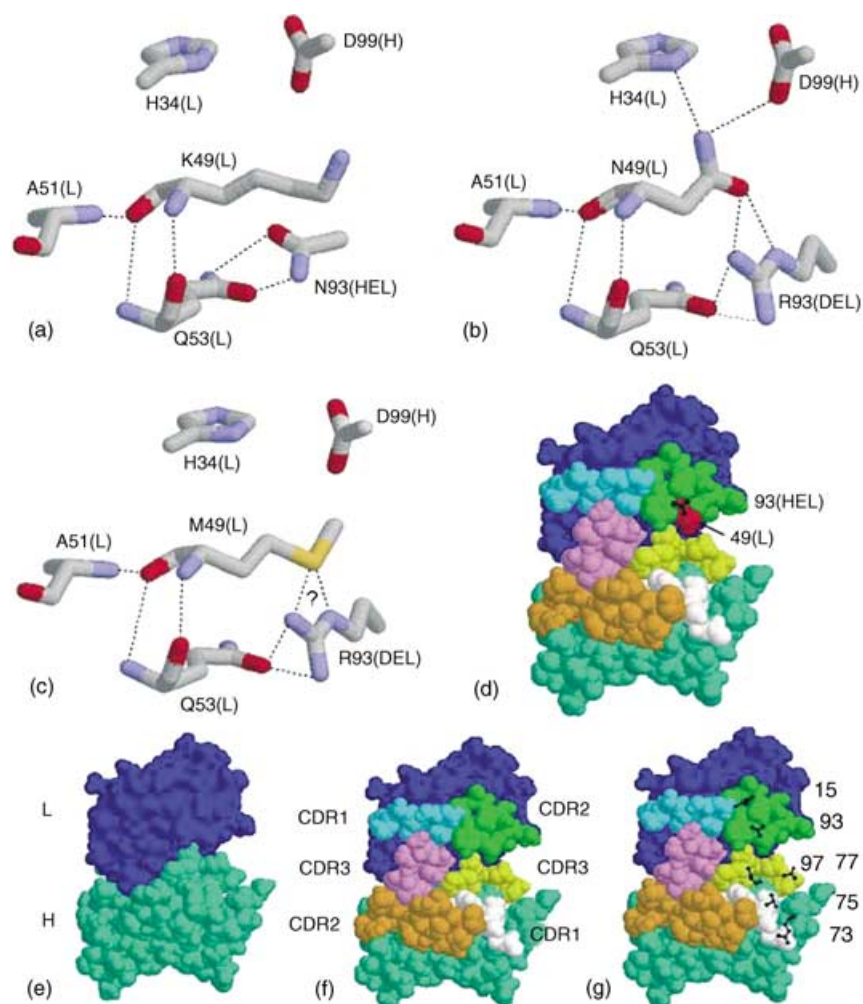


**Figure 6.** Protein modelling of antibody–lysozyme interactions. (a) Area of the antigen-binding site showing details of the interactions between HEL and the mouse HyHEL-10 anti-HEL antibody, based on the crystal structure of the Fab–antigen complex.<sup>28</sup> (b) Model of the same region showing the effects of the LysV $\kappa$ 49→Asn mutation on the interaction between the maturation mutant antibody and DEL. (c) Model of the same region showing the effects of the LysV $\kappa$ 49→Met mutation on the interaction with DEL. (d–g) Views of the HyHEL-10 antigen-binding site seen perpendicularly to the antibody–antigen interface. (d) employs the colour scheme of (f) and shows the position of the interacting side chains of residues LysV $\kappa$ 49 (red) and the HEL Asn93 (superimposed in black). (e) The two V domains: VH in green and V $\kappa$  in blue. (f) As (e) with the positions of the CDR regions shown by different colours. V $\kappa$ : CDR1, pale blue; CDR2, grass green; CDR3, violet. VH: CDR1, white; CDR2, orange; CDR3, yellow. (g) The same as (f) except that the side chains of the six interface residues differing between HEL and DEL are superimposed in black. Their size is reduced in (d) and (g) for clarity and the residue number is indicated at the right-hand side.

the rearrangement of the CDR loop caused by the mutation of these canonical important residues.

### Endogenous germline genes

Because the primers were specific for the V $\kappa$ 23 and VH36-60 gene families, a few rearranged germline V $\kappa$  and VH genes were also cloned from some of the IgM<sup>+</sup>, PNA<sup>+</sup> GCs. More endogenous V $\kappa$ 23 and VH36-60 genes were cloned from the GCs of DEL-cOVA recipients (35%) than from HEL-cOVA immunized animals (3%), which probably reflects competition between the transgenic and endogenous B cells for the lower affinity antigen, DEL. The number of mutations in these

endogenous V genes was similar to the number of mutations observed in the transgenic light chains. An endogenous VH-gene (with different D and J regions), that was a constituent of a polyreactive antihistone IgM antibody (GenBank accession no: X63801), was independently cloned at days 9 and 14 from DEL-cOVA immunized mice. This VH region is not a documented germline gene<sup>11</sup> and has been shown previously to bind HEL.<sup>53</sup>

### DISCUSSION

In this study, we have demonstrated affinity maturation of germinal centre B cells responding to two defined protein

antigens at the cellular and molecular level directly *in vivo* using a novel adoptive transfer model. This *in vivo* system exploits the different affinities of the HyHEL-10 antigen receptor for the monomeric protein antigens, hen egg lysozyme ( $K_a = 4.5 \times 10^{10} \text{ M}^{-1}$ ) and duck egg lysozyme ( $K_a = 1.3 \times 10^7 \text{ M}^{-1}$ ) and the fact that their conjugation to chicken ovalbumin allows provision of T cell help by cOVA-specific D011.10 T cells.<sup>20,21</sup> Previous *in vitro* and *in vivo* studies have examined various individual components (clonal expansion, GC formation, affinity maturation) of the antibody response but to our knowledge no sequential detailed analysis of the overall process to a protein antigen has been performed. This system has allowed us to track, in detail, at the level of antigen-specific B cells *in vivo*, all of these molecular and cellular events that occur during the development of an antibody response in one integrated experimental system. Not only will this have implications for a variety of therapeutic approaches, but it also provides an ideal system for studying the mechanisms underlying somatic hypermutation *in vivo*.

To ensure that DEL coupled to cOVA can elicit B cell help from TCR Tg T cells, as reported previously for HEL, we examined the clonal expansion of Tg T and B cells. Tg T cells responded more slowly to immunization with DEL-cOVA than with the higher affinity antigen (HEL-cOVA). This slower T cell response could be due to the low affinity of the BCR for DEL, resulting in less efficient presentation to T cells and hence slower recruitment of T cell help.<sup>40</sup> Alternatively, the lower affinity of the BCR for DEL may lead to competition for antigen between B cells and other antigen-presenting cells such as dendritic cells for presentation to T cells. Comparison of the levels of endogenous anti-cOVA IgG1 and IgG2a produced in response to HEL and DEL-cOVA indicates that the latter interpretation may be correct (unpublished data). Previous *in vitro* work has shown that, as the affinity of the BCR increases, there is a corresponding diminution in the amount of soluble antigen required to trigger a response, until the ability to discriminate further increases in affinity disappears above  $10^{10} \text{ M}$ .<sup>54–56</sup> Our study demonstrates for the first time that discrimination between a moderate ( $K_a = 10^7 \text{ M}^{-1}$ ) and a high-affinity ( $K_a = 5 \times 10^{10} \text{ M}^{-1}$ ) antigen also occurs during antigen presentation *in vivo*.

As we demonstrated that T and B cell clonal expansion occurs with HEL-cOVA and DEL-cOVA we were next able to employ the system to examine somatic hypermutation. To date, somatic hypermutation has been investigated only in GCs responding to haptens, due to the complexity and heterogeneity of the immune response to protein antigens. Many more contacts occur at the Ab–protein interface, which covers a much larger area, hence the process of antigenic-selection may be very different during the response to a protein antigen compared with the anti-hapten response.

The overall mutation rate within the GCs of this adoptive transfer system was fairly low (0.4%) but was significantly higher than the PCR error rate (0.08%),<sup>57</sup> and comparable with mutation rates from other primary responses.<sup>45,58</sup> Characteristics associated with somatic hypermutation such as a bias towards transitions and intrinsic hotspots, were also observed in the B cell transgenes. These results confirm the findings of other workers,<sup>39</sup> who have also shown somatic hypermutation in

the HyHEL-10 V $\kappa$  transgene in Peyer's patches of intact MD4 mice. However, in this case the antigen driving the response was unclear.

Possible reasons why the mutation rate is low in the system we describe are numerous. First, the heavy and light chain transgene cassettes are present in multiple copies and cointegrated into the genome, but not at the endogenous Igh and Ig $\kappa$  loci, in the MD4 transgenic mouse strain.<sup>23</sup> Each Tg cassette contains a strong Ig promoter and the intronic enhancer, which are essential elements for the initiation of somatic hypermutation.<sup>59–61</sup> This study and previous work verify that the correct placement of the transgenes within the Ig locus is not critical for mutation.<sup>39,62–64</sup> However, the Ig heavy chain 3' enhancer downstream from the C $\mu$  region is not present. Prior work has indicated that the lack of a 3' heavy chain enhancer reduces the rate of somatic hypermutation,<sup>65,66</sup> which could explain the lower mutation rate observed in the heavy chain transgene compared with the  $\kappa$  transgene in which the 3' enhancer is present. Additionally, the V $\kappa$  and VH HyHEL-10 transgenes contain two and 13 nucleotide differences from the nearest germline genes, V $\kappa$ 23 and VH36-60, respectively.<sup>34</sup> Some of these are in mutational hotspots, which are therefore no longer available for targeting. Finally, the HyHEL-10 BCR displays a moderate affinity for DEL, hence the low accumulation of mutations could be explained by ongoing emigration of Tg B cells without the requirement for recycling, since they can receive adequate survival signals through the BCR. Some GCs contain many B cells that have acquired one or two unique mutations only, indicating that they do not contain numerous recycling B cells. Additionally, other experimental systems may be observing memory B cells, recycling through germinal centres for further rounds of mutation. The transgenic B cells are unable to develop into memory cells due to the absence of switch recombination sites.<sup>67</sup>

Having demonstrated somatic hypermutation, we next determined whether the changes observed would be predicted to lead to an increase in affinity for the antigens in question. Competitive inhibition studies demonstrated an increase in affinity of serum antibodies, produced by transgenic B cells, towards DEL in DEL-cOVA immunized mice. Strong evidence for selection of mutations that shift the affinity from HEL to DEL is provided by the systematic detection of the light chain framework region mutations, 49V $\kappa$  (Lysine  $\rightarrow$  Methionine/Asparagine) in different DEL-cOVA recipients. The CDRs of HyHEL-10 are very short and 49V $\kappa$  is adjacent to the CDRL2, such that lysine 49 is in the centre of the DEL/HyHEL-10 interface. Protein modelling and previous site-directed mutagenesis experiments demonstrate that these mutations enhance affinity for DEL. Light chain mutations, Lys49V $\kappa$   $\rightarrow$  Thr and Ser93V $\kappa$   $\rightarrow$  Asn, were targeted by site-directed mutagenesis<sup>25</sup> due to the observation that HyHEL-10 and HyHEL-8 monoclonal antibodies, which share the same heavy and light chain V-genes (V $\kappa$ 23, VH36-60), differed in their ability to bind lysozymes from several species of birds, due to the positions of their somatically mutated amino acid residues.<sup>68</sup> Four of the five somatically mutated amino acid residues which differ between the HH8 and HH10 light chains (V $\kappa$  residues 49, 74, 77, 93),<sup>34</sup> were present within DEL-cOVA GC B cells and these have been shown to increase affinity for DEL sevenfold

by chain recombination experiments.<sup>25</sup> The intrinsic V $\kappa$  mutational hotspots Ser74 and 77 may have a subtle effect on affinity, although they are distant from the antigen-binding site. Although protein modelling can suggest local changes in antibody structure, it is unable to predict co-operative alterations in structure between somatically mutated residues or long range effects.<sup>69,70</sup> Protein modelling of numerous other replacement mutations in the light chain did not reveal direct interactions with DEL. Most coding changes appeared to be neutral, conserving antibody-antigen interactions and antibody structure. Mutations that are neutral in terms of affinity may offer selective advantages towards secretion, folding and physical stability.<sup>71</sup>

The observation that the canonically important light chain residues, Ile29 and Gln90,<sup>50,51</sup> were independently mutated to Phe and Arg, respectively, in the HEL-cOVA and DEL-cOVA suggests the influence of selective pressure, although we do not have direct evidence for an effect on antigen binding.

Replacement mutations in GC B cells responding to HEL-cOVA did not appear to be selected as none were repeated independently. The affinity of HyHEL-10 for HEL ( $4.5 \times 10^{10} \text{ M}^{-1}$ ) is believed to be near the effective ceiling for antibodies as B cells expressing very high affinity receptors do not show a significant advantage over this threshold as measured by competition for antigen bound to FDCs<sup>72</sup> or improved antigen presentation to T cells.<sup>54</sup> Roost *et al.*<sup>73</sup> demonstrated that germline genes encoding antibodies with high affinity for vesicular stomatitis virus showed no affinity maturation over the course of the immune response. Recently, it has been shown that antibody fragments with femtomolar affinities can be evolved by mutagenesis *in vitro*, demonstrating that limitations imposed by the antibody architecture are not intrinsically responsible for the affinity ceiling.<sup>74</sup> Importantly, our data show that B cells expressing antigen-receptors close to their affinity threshold are capable of revising their specificity by somatic hypermutation and selection in response to a low-affinity, cross-reactive antigen. This capability would allow further repertoire development of high affinity memory B cells, which could be important during the immune response to a pathogen undergoing antigenic drift. However, this advantage is offset by the danger that a similar repertoire shift could result in switching from an anti-pathogen response towards a low-affinity, cross-reactive autoantigen (antigen mimicry). Remarkably, mutations in this *in vivo* system recur independently at identical residues indicating that the affinity maturation process within the immune response is extremely selective. The effects of individual point mutations on the affinity of the transgenic HyHEL-10 antibody towards HEL and DEL are currently being investigated using scFv antibody fragments and surface plasmon resonance.

To our knowledge, this is the first time that affinity maturation of the GC response to high and low affinity cross-reactive protein antigens has been followed through completely from the clonal expansion of B and T cells in germinal centres to the effects of somatic mutations on the interaction of the antigen-binding site with its epitope. This model also provides an ideal system for studying the mechanisms underlying somatic hypermutation *in vivo*.

## ACKNOWLEDGMENTS

We would like to thank Mrs K. Smith and Dr G. Sims for their help in training C.A. in the adoptive transfer and microdissection techniques, respectively. This work was supported by the Leverhulme Trust.

## REFERENCES

- 1 Revy P, Muto T, Levy Y *et al.* Activation-induced cytidine deaminase (AID) deficiency causes the autosomal recessive form of the hyper-IgM syndrome (HIGM2). *Cell* 2000; **102**:565–75.
- 2 Bonhomme D, Hammarstrom L, Webster D *et al.* Impaired antibody affinity maturation process characterizes a subset of patients with common variable immunodeficiency. *J Immunol* 2000; **165**:4725–30.
- 3 MacLennan ICM. Germinal centre. *Annu Rev Immunol* 1994; **12**:117–39.
- 4 Kosco-Vilbois MH, Bonnefoy J-Y, Chvatchko Y. The physiology of murine germinal centre reactions. *Immunol Rev* 1997; **156**:127–36.
- 5 Camacho SA, Kosco-Vilbois MH, Berek C. The dynamic structure of the germinal centre. *Immunol Today* 1998; **19**:511–4.
- 6 Berek C, Milstein C. The dynamic nature of the antibody repertoire. *Immunol Rev* 1988; **105**:5.
- 7 Berek C, Berger A, Apel M. Maturation of the immune response in germinal centres. *Cell* 1991; **67**:1121–9.
- 8 Neuberger MS, Milstein C. Somatic hypermutation. *Curr Opin Immunol* 1995; **7**:248–54.
- 9 Kelsoe G. V(D)J hypermutation and receptor revision: coloring outside the lines. *Curr Opin Immunol* 1999; **11**:70–5.
- 10 Liu Y-J, Arpin C. Germinal centre development. *Immunol Rev* 1997; **156**:111–26.
- 11 Kabat EA, Wu TT, Reid-Miller M, Perry HM, Gottesman KS. Sequences of proteins of immunological interest. Bethesda, MD: US Government Printing Office, 1987.
- 12 Milstein C, Neuberger MS, Staden R. Both DNA strands of antibody genes are hypermutation targets. *PNAS* 1998; **95**:8791–4.
- 13 Wagner SD, Neuberger MS. Somatic hypermutation of immunoglobulin genes. *Annu Rev Immunol* 1996; **14**:441–57.
- 14 Green NS, Lin MM, Scharff MD. Somatic hypermutation of antibody genes: a hot spot warms up. *Bioessays* 1998; **20**:227–34.
- 15 Neuberger MS, Ehrenstein MR, Koop F, Jolly CJ, Yelamos J, Rada C, Milstein C. Monitoring and interpreting the intrinsic features of somatic hypermutation. *Immunol Rev* 1998; **162**:107–16.
- 16 Griffiths GM, Berek C, Kaartinen M, Milstein C. Somatic mutation and the maturation of immune response to 2-phenyl oxazolone. *Nature* 1984; **312**:271–5.
- 17 Berek C. Molecular events during maturation of the immune response to oxazolone. *Nature* 1985; **316**:412–8.
- 18 Sharon J. Structural correlates of high antibody affinity-3 engineered amino acid substitutions can increase the affinity of an anti-paraazophenylarsenate antibody 200-fold. *PNAS* 1990; **87**:4814–7.
- 19 Newman MA, Mainhart CR, Mallett CP, Lavoie TB, Smith-Gill SJ. Patterns of antibody specificity during the BALB/c immune response to hen egg lysozyme. *J Immunol* 1992; **149**:3260–72.
- 20 Garside P, Ingulli E, Merica RR, Johnson JG, Noelle RJ, Jenkins MK. Visualisation of specific B and T lymphocyte interactions in the lymph node. *Science* 1998; **281**:96–9.
- 21 Smith KM, Pottage L, Thomas ER. *et al.* Th1 and Th2 CD4<sup>+</sup> T cells provide help for B cell expansion and antibody synthesis in a similar manner *in vivo*. *J Immunol* 2000; **165**:3136–44.
- 22 Tze LE, Baness EA, Hippen KL, Behrens TW. Ig light chain receptor editing in anergic B cells. *J Immunol* 2000; **165**:6796–802.
- 23 Goodnow CC, Crosbie J, Adelstein S *et al.* Altered immunoglobulin expression and functional silencing of self-reactive B lymphocytes in transgenic mice. *Nature* 1988; **334**:676–82.

- 24 Goodnow CC. Transgenic mice and analysis of B-cell tolerance. *Annu Rev Immunol* 1992; **10**:489–518.
- 25 Lavoie TB, Drohan WN, Smith-Gill SJ. Experimental analysis by site-directed mutagenesis of somatic mutation effects on affinity and fine specificity in antibodies specific for lysozyme. *J Immunol* 1992; **148**:503–13.
- 26 Fischer MB, Goerg S, Shen L, Prodeus AP, Goodnow CC, Kelsøe G, Carroll MC. Dependence of germinal centre B cells on expression of CD21/CD35 for survival. *Science* 1998; **280**:582–5.
- 27 Smith-Gill SJ, Mainhart CR, Lavoie TB, Feldmann RJ, Drohan W, Brooks BR. A three dimensional model of an anti-lysozyme antibody. *J Mol Biol* 1987; **194**:713–24.
- 28 Padlan EA, Silvertown EW, Sheriff S, Cohen GH, Smith-Gill SJ, Davies DR. Structure of an antibody-antigen complex: crystal structure of the HyHEL-10 Fab-lysozyme complex. *PNAS* 1989; **86**:5938.
- 29 Lavoie TB, Kam-Morgan LNW, Hartman AB *et al.* Structure-Function Relationships in High Affinity Antibodies to Lysozyme, 1st edn. New York: Adenine Press, Inc., 1989
- 30 Smith-Gill SJ, Wilson AC, Potter EM, Prager RJ, Feldmann RJ, Mainhart CR. Mapping the antigenic epitope for a monoclonal antibody against lysozyme. *J Immunol* 1982; **128**:314–22.
- 31 Morsky P. Turbimetric determination of lysozyme with *Micrococcus lysodeikticus* cells. *Anal Biochem* 1983; **128**:77–85.
- 32 Murphy KM, Heimberger AB, Loh DY. Induction by antigen of intrathymic apoptosis of CD4<sup>+</sup>CD8<sup>+</sup> TCRlo thymocytes *in vivo*. *Science* 1990; **250**:1718–21.
- 33 Haskins K, Kubo R, White J, Pigeon M, Kappler J, Marrack P. The major histocompatibility complex-restricted antigen receptor on T cells. 1. Isolation with a monoclonal antibody. *J Exp Med* 1983; **157**:1149–69.
- 34 Lavoie TB, Mohan S, Lipschultz CA *et al.* Structural differences among monoclonal antibodies with distinct fine specificities and kinetic properties. *Mol Immunol* 1999; **36**:1189–205.
- 35 Chardes T, Villard S, Ferrieres G, Piechaczyk M, Cerutti M, Devauchelle G, Pau B. Efficient amplification and direct sequencing of mouse variable regions from any immunoglobulin gene family. *FEBS Letts* 1999; **452**:386–94.
- 36 Koop F, Richards JE, Durfee TD *et al.* Analysis and comparison of the mouse and human immunoglobulin heavy chain JH-C $\epsilon$ -C $\gamma$  locus. *Mol Phylogenet Evol* 1996; **5**:33–49.
- 37 Max EE, Maizel JV, Leder P. The nucleotide sequence of a 5.5-kilobase DNA segment containing mouse kappa immunoglobulin J and C regions genes. *J Biol Chem* 1981; **256**:5116–20.
- 38 Smith-Gill SJ, Hamel PA, Lavoie TB, Dorrington KJ. Contributions of immunoglobulin heavy and light chains to antibody specificity for lysozyme and two haptens. *J Immunol* 1987; **139**:4135–44.
- 39 Bemark M, Sale JE, Kim H-J, Berek C, Cosgrove RA, Neuberger MS. Somatic hypermutation in the absence of DNA-dependent protein kinase catalytic subunit (DNA-PKcs) or recombination-activating gene (RAG) 1 activity. *J Exp Med* 2000; **192**:1509–14.
- 40 Lanzavecchia A. Antigen specific interactions between T and B cells. *Nature* 1985; **314**:537–9.
- 41 Shih T-AY, Meffre E, Roederer M, Nussenzweig MC. Role of BCR affinity in T-cell-dependent antibody responses *in vivo*. *Nature Immunol* 2002; **3**:570–5.
- 42 Jacob J, Praylepa J, Miller C, Kelsøe G. *In situ* studies of the primary immune response to (4-hydroxy-3-nitrophenyl) acetyl. III. The kinetics of V region mutation and selection in germinal centre B-cells. *J Exp Med* 1993; **178**:1293–307.
- 43 Ziegner M, Steinhauser G, Berek C. Development of antibody diversity in single germinal centres: selective expansion of high affinity variants. *Eur J Immunol* 1994; **24**:2393–400.
- 44 Jacob J, Kelsøe K. Intracloonal generation of antibody in germinal centres. *Nature* 1991; **354**:389.
- 45 Vora KA, Tumas-Brundage K, Manser T. Contrasting the *in situ* behavior of a memory B cell clone during primary and secondary immune responses. *J Immunol* 1999; **163**:4315–27.
- 46 Jacob J, Kelsøe G. *In situ* studies of the primary immune response to (4-hydroxyl-3-nitrophenyl) acetyl. 2. A common clonal origin for periarteriolar lymphoid sheath-associated foci and germinal centres. *J Exp Med* 1992; **176**:679–87.
- 47 Wan W-Y, Milner-White EJ. A recurring two-hydrogen bond motif incorporating a serine or threonine residue is found both at alpha-helical N termini and in other situations. *J Mol Biol* 1999; **286**:1651–62.
- 48 Wan W-Y, Milner-White EJ. A natural grouping of motifs with an aspartate or asparagine residue forming two hydrogen bonds to residues ahead in sequence: their occurrence at alpha-helical N termini and in other situations. *J Mol Biol* 1999; **286**:1633–49.
- 49 Tsumoto K, Ogasahara K, Ueda Y, Watanabe K, Yutani K, Kumagai I. Role of Tyr residues in the contact region of anti-lysozyme monoclonal antibody HyHEL-10 for antigen binding. *J Biol Chem* 1995; **270**:18551–7.
- 50 Chothia C, Lesk AM. Canonical structures for the hypervariable regions of immunoglobulins. *J Mol Biol* 1987; **196**:901–17.
- 51 Chothia C, Lesk AM, Tramontano A *et al.* Conformations of immunoglobulin hypervariable regions. *Nature* 1989; **342**:877–83.
- 52 Martin ACR. Accessing the Kabat antibody sequence database by computer. *Proteins: Structure, Function Genet* 1996; **25**:130–3.
- 53 Novick HE, Fasy TM, Losman MJ, Monestier M. Polyreactive IgM antibodies generated from autoimmune mice and selected for histone binding activity. *Int Immunol* 1992; **4**:1103–11.
- 54 Batista FD, Neuberger MS. Affinity dependence of the B cell response to antigen: a threshold, a ceiling and the importance of off-rate. *Immunity* 1998; **8**:751–9.
- 55 Guermonprez P, England P, Bedouelle H, Leclerc C. The rate of dissociation between antibody and antigen determines the efficiency of antibody-mediated antigen presentation to T cells. *J Immunol* 1998; **161**:4542–8.
- 56 Kouskoff V, Famiglietti S, Lacaud G *et al.* Antigens varying in affinity for the B-cell receptor induce differential B lymphocyte responses. *J Exp Med* 1998; **188**:1453–64.
- 57 Sims GP, Shiono H, Wilcox N, Stott DI. Somatic hypermutation and acetylation of B cells in thymic germinal centers responding to acetylcholine receptor in *Myasthenia gravis*. *J Immunol* 2001; **167**:1935–44.
- 58 Liu A, Jena PK, Wyszocki LJ. Tracing the development of single memory-lineage B cells in a highly defined immune response. *J Exp Med* 1996; **183**:2053.
- 59 Betz AG, Milstein C, Gonzalez-Fernandez A, Pannell R, Larson T, Neuberger MS. Elements regulating somatic hypermutation of an immunoglobulin k gene: critical role for the intron enhancer/matrix attachment region. *Cell* 1994; **77**:239–48.
- 60 Storb U, Peters A, Klotz E *et al.* Cis-acting sequences that affect somatic hypermutation of Ig genes. *Immuno Rev* 1998; **162**:153–60.
- 61 Wabl M, Cascalho M, Steinberg C. Hypermutation in antibody affinity maturation. *Curr Opin Immunol* 1999; **11**:186–9.
- 62 Betz AG, Rada C, Pannell R, Milstein C, Neuberger MS. Passenger transgenes reveal intrinsic specificity of an antibody hypermutation mechanism: clustering, polarity and specific hotspots. *Proc Natl Acad Sci USA* 1993; **90**:2385–8.
- 63 Yelamos J, Klix N, Goyenechea B *et al.* Targeting of non-Ig sequences in place of the V segment by somatic hypermutation. *Nature* 1995; **376**:225–9.
- 64 Peters A, Storb U. Somatic hypermutation of immunoglobulin genes is linked to transcription initiation. *Immunity* 1996; **4**:57–65.

- 65 Bachl J, Wabl M. Enhancers of hypermutation. *Immunogenetics* 1996; **45**:59–64.
- 66 Bachl J, Olsson C, Chitkara N, Wabl M. The Ig mutator is dependent on the presence, position, and orientation of the large intron enhancer. *PNAS* 1998; **95**:2396–9.
- 67 Kinoshita K, Honjo T. Linking class-switch recombination with somatic hypermutation. *Mol Cell Biol* 2001; **2**:493–503.
- 68 Smith-Gill SJ, Mainhart CR, Lavoie TB, Rudikoff S, Potter M. VL-VH expression by monoclonal antibodies recognizing avian lysozyme. *J Immunol* 1984; **132**:963–7.
- 69 Dall'Acqua W, Goldman ER, Lin W *et al.* A mutational analysis of binding interactions in an antigen–antibody protein–protein complex. *Biochemistry* 1998; **37**:7981–91.
- 70 Yang PL, Schultz PG. Mutational analysis of the affinity maturation of antibody 48G7. *J Mol Biol* 1999; **294**:1191–201.
- 71 England P, Nageotte R, Renard M, Page A-L, Bedouelle H. Functional characterization of the somatic hypermutation process leading to antibody D1.3, a high affinity antibody directed against lysozyme. *J Immunol* 1999; **162**:2129–36.
- 72 Batista FD, Neuberger MS. B cell extract and present immobilized antigen: implications for affinity discrimination. *EMBO J* 2000; **19**:513–20.
- 73 Roost HP, Bachmann MF, Haag A, Kalinke U, Pliska V, Hengartner H, Zinkernagel RM. Early high affinity neutralizing anti-viral IgG responses without further overall improvements of affinity. *PNAS* 1995; **92**:1257–61.
- 74 Boder ET, Midelfort KS, Wittrup KD. Directed evolution of antibody fragments with femtomolar antigen-binding affinity. *PNAS* 2000; **97**:10701–5.